A facile low-temperature route for preparing monodisperse Mn_3O_4 nanopolyhedrons from amorphous MnO_2 nanoparticles

Shuping Zhang*, Wei Liu**, Jie Ma*, and Yan Zhao***

** College of Science, University of Shanghai for Science &Technology, majie@usst.edu.cn*
***College of Environment & Construction, University of Shanghai for Science &Technology*
****School of Medical Instrument and Food Engineering, University of Shanghai for Science &Technology*

ABSTRACT

A simple hydrothermal route has been utilized for preparing monodisperse tetragonal Mn_3O_4 nanocrystal from new-made amorphous MnO_2 nanomaterials. The MnO_2 nanomaterials with its mother solution are directly used as precursor without any pre-separation or pre-disposal process. The as-obtained samples are characterized by XRD, FTIR, SEM, TEM, SAED, and VSM. The two stages reaction procedures are clarified with the hydrothermal treatment time increasing. First stage is the formation of MnOOH nanorods and Mn_3O_4 nanoparticles mixture. Another is the transformation from MnOOH nanorods to monodisperse Mn_3O_4 polyhedron nanoparticles. The VSM results indicate the excellent superparamagnetic character of as-obtianed Mn_3O_4 polyhedron nanoparticles at room-temperature.

Keywords: Nanomaterial; Mn_3O_4; Hydrothermal; MnO_2; superparamagnetic.

1. INTRODUCTION

Manganese oxides and oxyhydroxides have been paid more attentions as important multifunctional and extensive utilized-prospects materials. Manganese oxides nano-materials show excellent supercapacitive characteristics with high values of specific capacitance, catalysis, magnetic properties[1-3]. Moreover, manganese oxides are in abundance and low cost as well as environmentally benign nature[4]. Mn_3O_4 shows an effective catalysis for selective reduction of nitrobenzene and the decomposition of NO_x [5]. Mn_3O_4 is also used to produce manganese zinc ferriteas soft magnetic materials and lithium manganese oxides as rechargeable electrode materials[6]. MnOOH has been used for adsorption of chemical and radioactive wastes and for oxidation of non-biodegradable

For preparation of manganese oxides, various method have been developed and exploited, such as hydrothermal [8], sol-gel[9], electro-deposition[10], solvothermal[11], etc. As we known, though $KMnO_4$ as a solvothermal precursor has been widely adopted for synthesizing Mn_3O_4 nanomaterials, most reports have just focused on obtained a single targeted product and neglected reaction intermediate processes[11]. Consequently, the ambiguous reaction mechanism is necessary to be elucidated

For clarifying the reaction procedures in water-ethanol solvothermal system, we divide the whole reaction processes into room-temperature mixture reaction stage and solvothermal treatment stage, rather than directly treatment of the mixture of $KMnO_4$ and water-ethanol in hydrothermal system. By this alternative route, not only reaction intermediate products including amorphous MnO_2 nanoparticles, and MnOOH nanorods are acquired, but also it is disclosed MnO_2 could be directly utilized as precursor to prepare lower valance manganese oxides or oxyhydroxides nanomaterials under appropriate reducer assistance. The samples obtained at different stages were characterized by XRD, FTIR, SEM, TEM and SAED. Furthermore, the room-temperature magnetic properties of typical samples were measured by VSM。

2. EXPERIMENTAL

MnO_2 amorphous nanomaterial was synthesized according to the reference[12]. For preparing Mn_3O_4 nanomaterial, the solution was not re-newly made by fresh Mn_3O_4 amorphous nanomaterial, but directly used the turbid mixture contained amorphous MnO_2 in hydrothermal approach. Take a typical example, 20 ml above-mentioned mixture was transferred into Teflon-lined stainless-steel 25 ml capacity autoclave. The autoclave was sealed and maintained constantly at 160 °C for 24 h in a digital-controlled constant temperature oven. Then autoclave was cooled to room-temperature naturally. The yellow-brownish precipitate was centrifuged and washed extensively with de-ionized water and ethanol in turn many times. Finally, the obtained products were dried under vacuum at 60 °C for storage and further characterization.

The product were characterized by X-ray powder diffraction (XRD, Bruker D8, Germany) equipped with graphite monochromatized Cu Ka radiation (λ = 1.54056 Å), employing a scanning rate of 0.02° s^{-1}, in the 2θ ranges from 10° to 70°. Infrared spectra (4000–400 cm^{-1}) were recorded by a Nicolet 5DX FTIR spectrometer with 1 cm^{-1} resolution. The micro-morphologies and nanostructure of products were inspected by scanning electron microscopy (SEM, Philip XL30, Holland), transmission electron microscopy (TEM, Hitachi, H800EM, Japan) with selected area electron diffraction (SAED). The room-temperature magnetic properties of typical samples are characterized by vibrating sample magnetometer (VSM, Lake Shore 735VSM, USA) in the range of -5000 -5000 Oe.

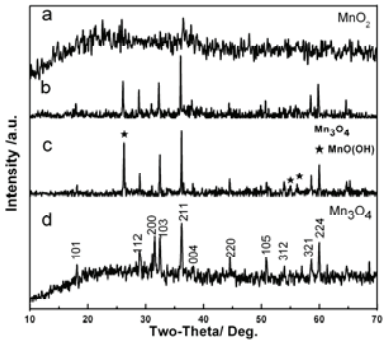

Fig.1 The XRD patterns of a) at room-temperature; b) obtained via hydrothermal at 160 ºC for 12 h; c) via hydrothermal at 160 ºC for 12 h without CTAB; d) via hydrothermal at 160 ºC for 24 h.

3. RESULTS AND DISCUSSIONS

The XRD patterns of the samples obtained by different routes are investigated and laid out in Figure 1. Figure 1a shows the amorphous material sample obtained via solutions route at room-temperature. The material is confirmed as MnO_2 by element analysis and FTIR spectra shown in figure 2a, which is according with the literature[12]. The pattern shown in figure 1b exposes the sample obtained via hydrothermal at 160 ºC for 12 h is composed of monoclinic phase γ-MnOOH (JCPDS 41-1379) and tetragonal phase Mn_3O_4 (JCPDS 24-0734 hausmannite-mine type). The diffraction peaks of γ-MnOOH are signed by "★" in the pattern. When hydrothermal process was lasted at 160 ºC for 24h, the pure Mn_3O_4 nanomaterial was demonstrated by sample's XRD pattern shown the figure 1d. The cell parameters of the product are corrected as a = 5.749(2) Å and c = 9.455(1) Å. Above results suggest that the reaction from MnO_2 to Mn_3O_4 nanomaterial can be accomplished via hydrothermal at 160 ºC for 24 h. Meanwhile, The series of XRD patterns also explored that this transformational processes from MnO_2 to Mn_3O_4 nanomaterial can be divide two stages including the transfer from MnO_2 to γ-MnOOH intermediate, and then to Mn_3O_4 nanomaterial. In other words, the Mn^{4+} is firstly reduced to Mn^{3+}, and then part of Mn^{3+} is further reduced to Mn^{2+} in the procedures. For investigating the function of additive CTAB, the hydrothermal process was also performed at similar conditions except without CTAB at 160 ºC for 12 h. The XRD pattern of the sample indicate the product is made up of γ-MnOOH and Mn_3O_4 nanomaterials (**figure 1c)**, which is also approved by the FTIR spectrum shown in figure 2c.

FTIR spectra were inspected and listed in figure 2. When the sample was obtained at room-temperature, the spectrum was resembled with that of MnO_2 shown in figure 2a. The spectrum displayed a strong absorbance band at 523 cm-1 due to Mn-O vibrations of MnO_2. The bands at 2931 and 2860 cm^{-1} indicated some CTAB absorbed by the amorphous MnO_2 nanomaterial. The peaks at 1080 to 1160 cm^{-1} were attributed to the OH bending modes. Another peak at 2089 cm^{-1} considered as a combination band of the OH stretching mode at 2680 cm^{-1} and the excited lattice mode at 592 cm^{-1} was also observed. The belonged to γ-MnOOH. The peaks below 627 cm^{-1} could be attributed to the Mn–O vibrations. The results indicated that the γ-MnOOH was existed in the sample, which was consistent with some studies of Kohler et al [13] and Sharma et al [14]. Meanwhile, the characteristic FTIR absorption peaks of the Mn_3O_4 were appeared in the spectrum with the bands at 634, 531 and 416 cm^{-1}. The FTIR spectra of the as-obtained sample by hydrothermal treatment 24 h with CTAB was presented in figure 2d. Three main absorption peaks were inspected in the range of 400-650 cm^{-1}, the band 634 cm^{-1} was characteristic of Mn-O stretching modes in tetrahedral sites, whereas vibration frequency at 531 cm^{-1} was attributed to the distortion vibration of Mn-O in an octahedral environment. The third vibration band at 416 cm^{-1} corresponded to the vibration of manganese species (Mn^{3+}) in an octahedral site, and 1632 and 1402 cm^{-1} bands were normally attributed to O-H bending vibrations combined with Mn atoms [15].

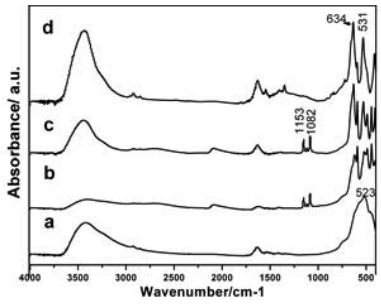

Fig. 2 The FTIR spectra of a) at room-temperature; b) via hydrothermal at 160 ºC for 12h; c) via hydrothermal at 160 ºC for 12h without CTAB; d) via hydrothermal at 160 ºC for 24 h.

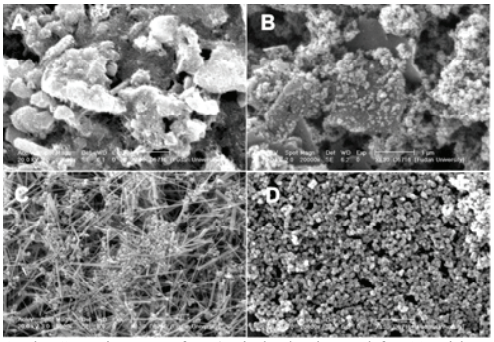

Fig. 3 The SEM images of a. a) via hydrothermal for 12 without CTAB; b) at room-temperature; c) via hydrothermal 12h; d) via hydrothermal 24 h.

Figure 3 showed SEM micrographs of the products obtained via different routes. Figure 3A exhibited the sample was consisted of seriously agglomerating nanoparticles and nanorods, which was synthesized via hydrothermal treatment without CTAB at 160 ºC for 12 h. The obtained MnO_2 sample revealed loose or agglomerated nano-multiceps with size around 30-50 nm (figure 3B). When the mixture was treated via hydrothermal with CTAB at 160 ºC for 12 h, the micrographs in figure 3C exposed

the sample was made up of γ-MnOOH nanorods and Mn_3O_4 nanoparticles, which was proved by SAED patterns shown in figure 4. Compared figure 3c to 3a, with some CTAB assistance, more regular product with lower agglomeration was synthesized. It should be contributed to the interaction inhibited the crystal aggregation between CTAB and crystal surface. With the hydrothermal treatment enhanced to 24 h, the sample was composed of uniform mono-disperse regular polyhedral nanoparticles with the size ca.50-60 nm shown in figure 3D.

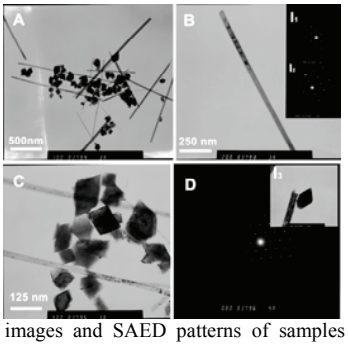

Fig. 4 The TEM images and SAED patterns of samples obtained via hydrothermal for 12h. A) Low magnification image; B) the single nanorod with its SAED patterns signed as I_1 and I_2; C) High magnification image; D the SAED pattern of the nanoparticle with its corresponding TEM image inserted

To further investigate crystal status of samples obtained hydrothermal treatment, the TEM and SAED were applied to inspect samples and typical micrographs and ED pattern were shown in figure 4 and figure 5, respectively. Figure 4 A and 4C showed two different magnification TEM images of the samples obtained at 12h, the sample was constitutes of nanorods with diameter ca.40 nm and polyhedron nanoparticles with the size about 60-80nm accordingly with figure 3C. The ED patterns and corresponding TEM image were exhibit in the figure 4 B and 4D, respectively. Two different crystal facet ED pattern of nanorods were shown in figure 4b as inserts I_1 and I_2, which is accordance with monoclinic phase γ-MnOOH calculated by crystal facet interspacing and correspond the diffraction direction of ED are as [1-2 1] and[011], respectively. The obvious contrast diffracted SAED pattern of representative nanoparticle indicated nanoparticles was belonged to the different structure with the nanorods, and its corresponding TEM image was inserted into figure 4D. By calculated of patterns, the sample was the tetragonal phase Mn_3O_4 structure. The diffraction direction of electron beam is along [001]. Above SAED patterns and TEM images further demonstrated that the sample was composed of different shape γ-MnOOH and Mn_3O_4.

The TEM image shown in figure 5 further indicated uniform polyhedron structure nanoparticles with the narrow size distribution between 50- 60nm. The typical SAED pattern was shown in figure 5D and its responding representation particle was inserted in the picture. The electron beam was ascertained as [010] direction and the *d* values of various crystal facets accord with them of tetragonal phase Mn_3O_4.

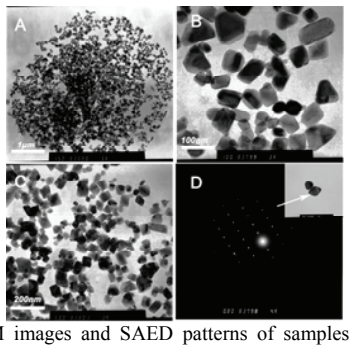

Fig. 5 The TEM images and SAED patterns of samples obtained via hydrothermal for 24h. A) ,B) and C) are different magnification image of the sample; D) the SAED pattern of the nanoparticle with its corresponding TEM image inserted in the picture.

Based on above inspected results, the pure Mn_3O_4 nanoparticles growth procedures can be demonstrated by the scheme 1 and described as follow: 1) The amorphous loose MnO_2 nano-multiceps formation. 2) During the hydrothermal treatment earlier stage, the mixture of MnO_2 is gradually turned into γ-MnOOH nanorods and Mn_3O_4 nanoparticles. 3) In the hydrothermal treatment later stage, the γ-MnOOH is gradually reduced to Mn_3O_4. The firstly stage is easily accomplished at room-temperature, for $KMnO_4$ shows strong oxidizability and oxidizes ethanol into aldehyde with the MnO_2 formation. For the CTAB as a surfactant is readily absorbed on surface of MnO_2 crystal nucleus, the crystal MnO_2 grow very slowly and loose structure is finally formed at low-temperature. The intention of keeping the reaction at room-temperature for 24h is that no residues $KMnO_4$ are insured. In the second stages, the formation of γ-MnOOH and Mn_3O_4 nanometerial should be attributed to the infirm oxidability and reducibility of MnO_2 and ethanol. Under hydrothermal treatment conditions at 160 ºC for 12 h, A part of amorphous MnO_2 particles are further reduced to γ-MnOOH by ethanol with the crystal shape transference from nano-multiceps to regular nanorods. Meanwhile, other parts of MnO_2 particles are directly reduced to Mn_3O_4 nanoparticles with the crystal phase and appear transformation. In the finally stage, with the treatment time changed from 12 h to 24h, the γ-MnOOH is further reduced and changed to Mn_3O_4 in water-ethanol system. Meanwhile, nanorods completely disappear and form the single component nanoparticles. The formation of Mn_3O_4 nanoparticles in the hydrothermal system are reasonable illuminated by a dissolution–recrystallization[16] and cleavage-decomposition mechanism[17]. Compared to the sample via directly used $KMnO_4$ and water-ethanol (1:1) as hydrothermal precursors at 160 ºC for 12 without CTAB, the above indirectly reaction process is more facilely obtained lower aggregative nanomaterial.

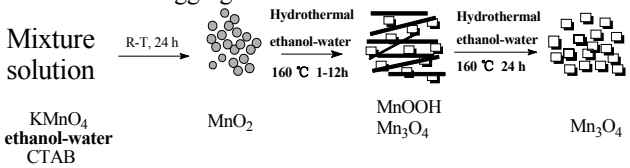

Scheme 1 The reaction processes for forming of Mn_3O_4 nanoparticles via hydrothermal treatment.

For further distinguishing as-obtained MnO_2, intermediate product, and pure Mn_3O_4 nanomaterials, the room-temperature magnetic properties of them are characterized by VSM and obtained hysteresis loops are shown in figure 6. The M–H curves show that the loops of MnO_2 and mixture intermediate are linear with the field with coercivity about 17.107 and 20.059 Oe, respectively. Contrarily, the loop of the Mn_3O_4 nanomaterial reveals an obvious small bend magnetic field in the range of -1500 to 1500 Oe with coercivity about 9.6798 Oe. Compared to the MnO_2 precursor, the coercivity of pure Mn_3O_4 nanoparticles is declined to half, however, the coercivity of the mixture intermediate is slightly increased. This result should be attributed to the transformation of crystal structure, valence of Mn and shape of samples. Because the no hysteresis shown in Mn_3O_4 sample M–H behavior is like in the case of paramagnetism and the magnetization never gets saturated even at very high applied field, this state of the ferromagnetism is called 'superparamagnetism[18], indicating the superparamagnetic character of the Mn_3O_4 samples. When ferromagnetic systems loose their multidomain character, they are then termed as single domain with their magnetic spins aligned along one of the easy directions of magnetization. Compared with the report of Ozkaya et al [19], the bend existed in the loop of Mn_3O_4 nanomaterials should be contributed to different size and shape come from crystallization condition of the product.

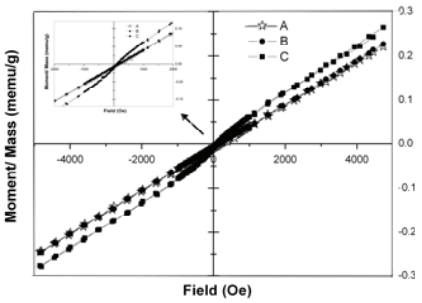

Fig. 6 The room-temperature magnetic properties of samples. A) the mixture of MnOOH nanorods and Mn_3O_4 nanoparticles; B) amorphous MnO_2 nanoparticles; C) Mn_3O_4 nanoparticles. Inset: the magnified pattern of the low field region.

4. CONCLUSIONS

In this work, Mn_3O_4 nanoparticles have been successfully obtained via a facile hydrothermal treatment, in which new-made amorphous MnO_2 nanoparticles with its mother-solution are directly used as precursor. This work firstly shows that MnO_2 can be transferred into monodisperse Mn_3O_4 polyhedron nanoparticles with the size around 60-80 nm via a suitable hydrothermal process, and reveals MnOOH nanorods is important intermediate. During the formation of Mn_3O_4 nanoparticles, the crystal phase growth and shape change are reasonable illuminated by a dissolution–recrystallization mechanism. The as-prepared Mn_3O_4 nanoparticles show super- paramagnetic character due to the small size effect.

ACKNOWLEDGEMENTS

The authors are thankful to the National '11th-five' Science & Technology Plan Key Project Foundation (No.2007BA62B04), the Shanghai International Cooperation Foundation (No. 073458014) and the Shanghai excellent young Foundation for financial support.

REFERENCES

[1] Zhang H, Cao G, Wang Z, Yang Y, Shi Z, Gu Z. Nano Letters 8, 2664, 2008
[2] Subramanian V, Zhu H, Vajtai R, Ajayan PM, Wei B. J. Phys. Chem. B 109, 20207, 2005
[3] Cui X, Liu G, Lin Y. Nanomedic Nanotech Bio Medic 1, 130, 2005
[4] Bakenov Z, Wakihara M, Taniguchi I.. J Solid State Electrochem 12, 57, 2008
[5] Han YF, Chen F, Zhong Z, Ramesh K, Chen L, Jian D, Ling WW. Chem Eng J 134, 276, 2007
[6] Pan'kov VV. Ceram. Int. 14, 87, 1988
[7] Rabiei S, Miser DE, Lipscomb J A, Saoud K, Gedevanishvili S, Rasouli F. J Mater Sci 40: 4995, 2005
[8] Shen X F, Ding Y S, Hanson J C, Aindow M, Suib S L. J Am Chem Soc. 128, 4570, 2006
[9] Ching S, Petrovay DJ, Jorgensen ML, Suib SL. (Inorg Chem 36, 883, 1997
[10] Nakayama M, Tagashira H. Langmuir 22, 3864, 2006
[11] Zhang W, Yang Z, Liu Y, Tang S, Han X, Chen M. J. Crystal Growth 263, 394, 2004
[12] Subramanian V, Zhu H, Wei B. Chem Phys Lett 453, 242, 2008
[13] Kohler T, Armbrustor T, Libowitzky E. J. Solid State Chem. 133, 486, 1997
[14] Sharma P K, Whittingham MS. Mater. Lett. 48: 319, 2001
[15]Wang XL, Yuan AB, Wang YQ. J Power Sources 2, 1007. 2007
[16] Ma J, Wu Q, Ding Y. J Nanopart Res 10: 775, 2008
[17] Chen Y, Zhang Y, Yao QZ, Zhou G T, Fu S, Fan H. J Solid State Chem 180, 1218, 2007
[18] Liu C, Rondinone A J, Zhang ZJ. Pure Appl Chem 72, 37, 2000
[19] Ozkaya T, Baykal A, Kavas H, Köseoğlu Y, Toprak MS. Physica B 403: 3760, 2008